Electronic Supplementary Material (ESI) for Analyst.
This journal is © The Royal Society of Chemistry 2014

Supporting Information for

13C-Engineered Carbon Quantum Dots for *in vivo* Magnetic Resonance and Fluorescence Dual-Response

Yang Xu,[a] Yu-Hao Li,[b] Yue Wang,[b] Jian-Lin Cui,[b] Xue-Bo Yin,[a,*] Xi-Wen He,[a] and Yu-Kui Zhang[a,c]

[a] State Key Laboratory of Medicinal Chemical Biology, Collaborative Innovation Center of Chemical Science and Engineering (Tianjin), and Research Center for Analytical Sciences, College of Chemistry, Nankai University, Tianjin, 300071, China

[b] Key Laboratory of Animal Models and Degenerative Neurological Diseases (Tianjin), School of Medicine, Nankai University, Tianjin, 300071, China

[c] Dalian Institute of Chemical Physics, National Chromatographic R. & A. Center, Chinese Academy of Sciences, Dalian, 116011, China

*X,-B. Yin, College of Chemistry, Nankai University, Tianjin, 300071, China. Email: xbyin@nankai.edu.cn; Fax: +86-22-23503034.

Results and discussions

Characterization of ^{13}C- and ^{12}C-QDs. Fourier transform infrared (FTIR) and X-ray photoelectron spectroscopy (XPS) spectra reveal the groups in the two kinds of C-QDs. ^{12}C-QDs and ^{13}C-QDs have the almost same FTIR spectra (Fig. S1). Three strong bands at 1058, 1654 and 3377 cm^{-1} attributed to the C-O-C, C=O and –OH, respectively. [1] A low peak associated with amide (–CONH–) was found at 1768 cm^{-1}, indicating that the passivation agent, monoethanolamine (MEA), reacts with glucose.[1a,2] The XPS result shows the composition and function groups on C-QDs (Fig. S2). The C1s peak can be resolved into four peaks at 284.5, 285.8, 287.4, 288.6 eV, attributed to C-C, C-N, C-O, C=O, respectively. [3] The N1s peak of C-QDs can be observed with two peaks at 399.5 and 401.6 eV, which are associated with C-N-C and N-H groups.[3] The elemental analysis results (Table S1) show that 48.97 % C, 6.75 % H, 10.01 % N, and 34.27 % O (calculated) in^{12}C-QDs; 52.16 % C, 6.20 % H, 9.77 % N, and 31.87 % O (calculated) in ^{13}C-QDs. Those spectra reveal that ^{12}C- and ^{13}C-QDs have similar composition and surface groups.

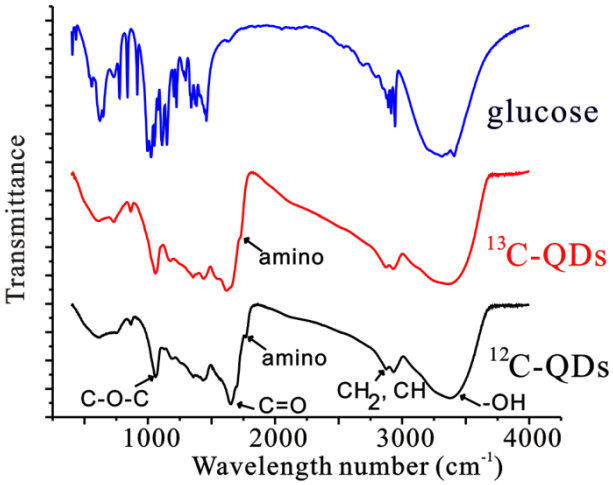

Fig. S1. IR spectrum of glucose, ^{13}C-QDs, and ^{12}C-QDs.

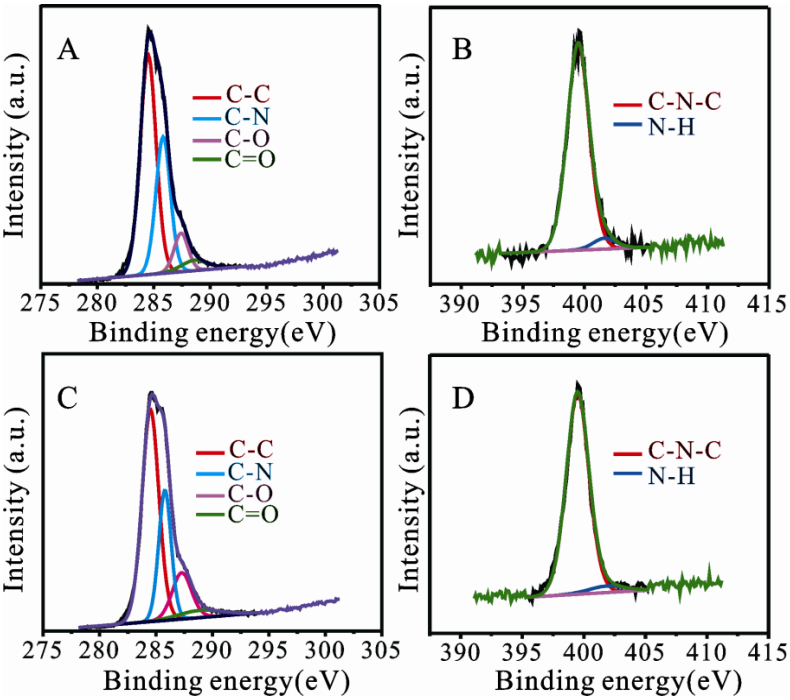

Fig. S2. XPS C_{1s} and N_{1s} spectra of (A, B) ^{12}C-QDs and (C, D) ^{13}C-QDs.

Table S1. Elemental analysis of C-QDs

Sample	C/%	H/%	N/%	O/% (calculated)
^{12}C-QDs	48.97	6.75	10.01	34.27
^{13}C-QDs	52.16	6.20	9.77	31.87

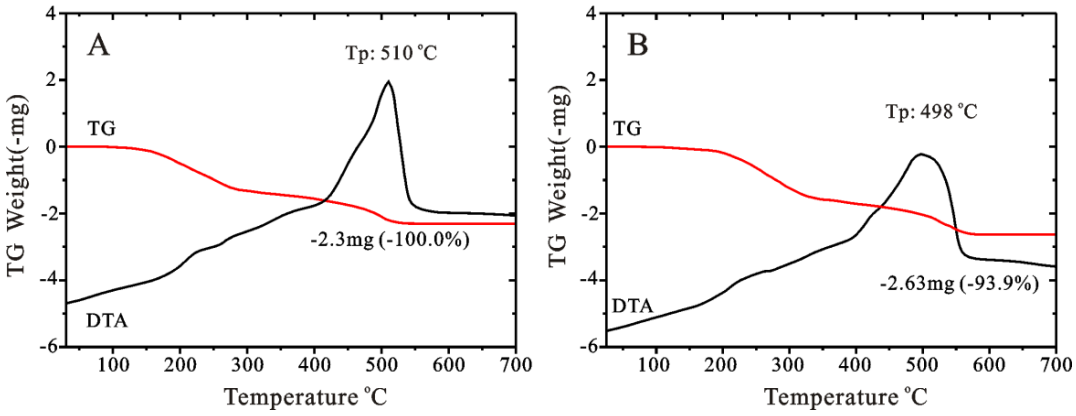

Fig. S3 . TGA & DTA trace in air of (A) ^{12}C-QDs and (B) ^{13}C-QDs.

Quantum yields (QY) of C-QD. Quantum yields of both of C-QDs were determined according to a slope method with quinine sulfate in 0.1 M H_2SO_4 as a reference (QY = 54 %). The quantum yield of C-QDs were calculated with the following equation:

$$\Phi_x=\Phi_{st}(K_x/K_{st})(\eta_x/\eta_{st})^2$$

Where Φ is the quantum yield, K is the slope determined by the curves, and η is the refractive index. The subscript "st" refers to the referenced fluorophore with known quantum yield and "X" refers as the sample (C-QDs in this work) for the determination of quantum yield. In order to minimize re-absorption effects, absorption was kept below 0.05 at the excitation wavelength of 360 nm.

Table S2. The QY of C-QDs.

Serial	quinine sulfate	^{12}C-QDs	^{13}C-QDs
K	11635	2737	3679
η	1.33	1.33	1.33
Φ/%	54	12.7	17.1

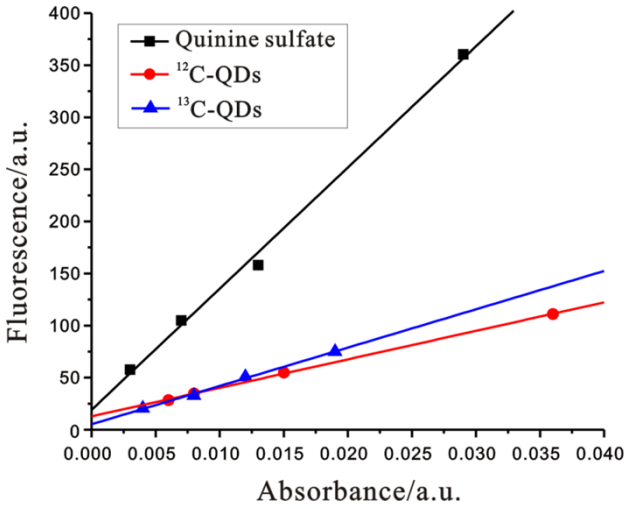

Fig. S4. The linear fluorescence-absorbance curve of C-QDs.

Upconversion emission and photo-stability of C-QDs. Upconversion emission was observed from the two kinds of C-QDs under excitation in the range of 680–880 nm (Fig. S5). Thus, C-QDs can be used for bio-imaging with NIR excitation similar to some rare earth materials, [4] which can decrease the effect from the auto-fluorescence and scattered light of animal tissue. Moreover, ^{13}C-QDs exhibited an excellent anti-photo-bleaching property using continuous UV light and high photo-stability in salt solution (Fig. S6). It implied that C-QDs can be used for the imaging without apparent signal decay along with the illuminated time at least within 60 min and changed salt concentration up to 1 M NaCl. C-QDs have been reported to show a stable emission after storage for 1 year. [5] It indicates that the storage decreases the surface defect and illustrates that the PL of C-QDs is governed by defect-derived mechanism. [6] Those merits make C-QDs potential as probes for *in vivo* imaging.

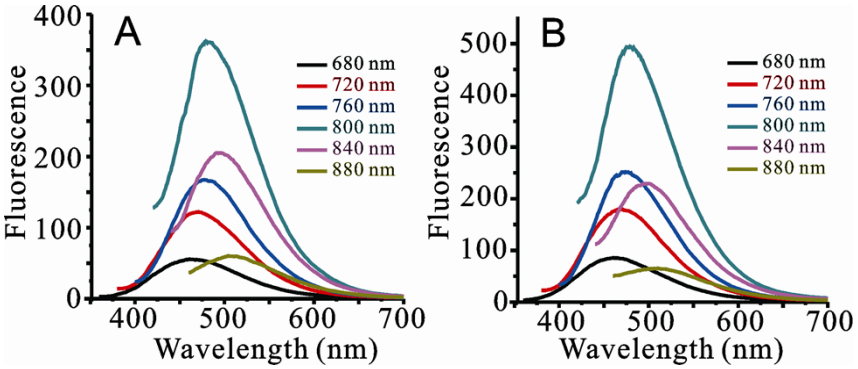

Fig. S5. The upconversion emission profiles of (A) ^{12}C-QDs and (B) ^{13}C-QDs.

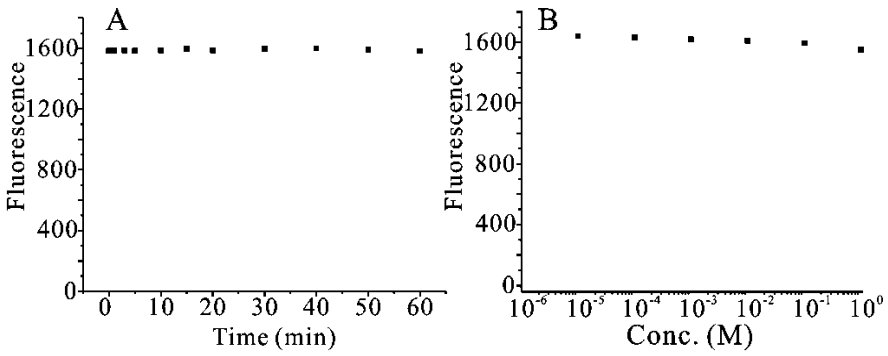

Fig. S6. (A) Time-dependent emission at different illumination time and (B) Salt concentration-dependent emission of ^{13}C-QDs with different concentration of sodium chloride.

Fluorescence imaging with ^{13}C-QDs as probe

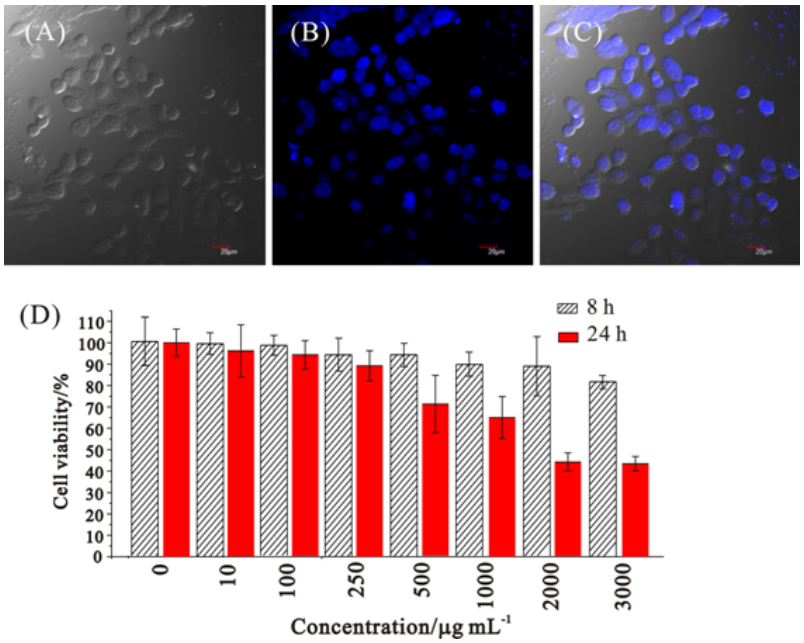

Fig. S7. Confocal images of 4T1 cells incubated with ^{13}C-QDs. (A) Bright field images; (B) fluorescence image under excitation at 405 nm; (C) merged images. (D) Cell viability of 4T1 cells incubated with ^{13}C-QDs. Data were presented as the mean ± the standard deviation (SD).

Biological toxicity of ^{13}C-QDs. Zebrafish at 72 hpf were incubated with ^{13}C-QDs at different concentration for 8 hours to test the biological toxicity of ^{13}C-QDs. More than 80 % and 60 % of zebrafish viability were observed after being incubated with 3.0 and 5.0 mg mL^{-1} ^{13}C-QDs, respectively, indicating the low toxicity of ^{13}C-QDs being suitable for *in vivo* imaging (Fig. S8).

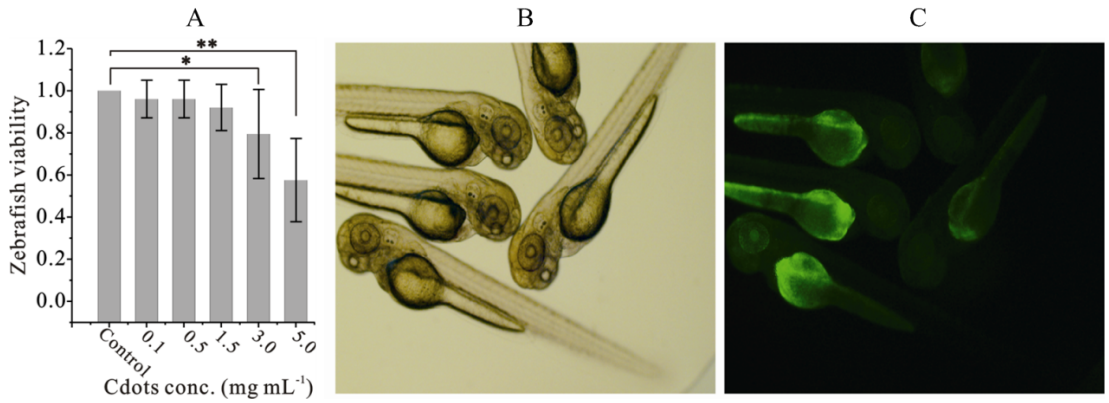

Fig. S8. Biological toxicity of the ^{13}C-QDs. (A) Effect of ^{13}C-QDs of different concentrations on the viability of zebrafish. Data presented as mean ±SD. (B) Bright field images and (C) fluorescence images of zebrafish after incubating with ^{13}C-QDs at 3.0 mg mL^{-1} level at 72 hpf. Data were presented as the mean ± the standard deviation (SD). * Denotes statistically significant difference P<0.1. ** Denotes statistically significant difference P<0.05 with the Students t-test.

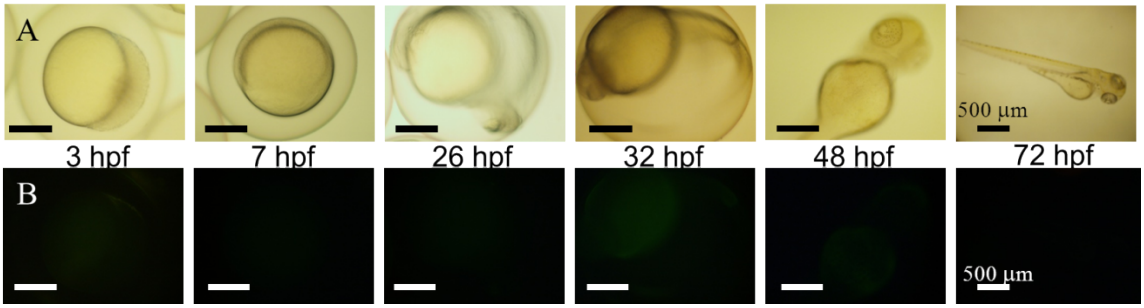

Fig. S9 (A) Bright-field and (B) fluorescence images of embryo without ^{13}C-QDs at the different stages: 3, 7, 26, 32, 48, and 72 hpf. Scale bar: 250 μm besides the marked.

Table S3. Fluorescence images of zebrafish (80 hpf) incubated with ^{13}C-QDs at different concentrations. (A) Whole zebrafish, (B) Front part of the body with head and yolk sac, (C) Rear part of the body, and (D) Enlarged image of the eye.

	a: control	b: 0.75 mg mL^{-1}	b: 1.0 mg mL^{-1}	d: 3.0 mg mL^{-1}
A		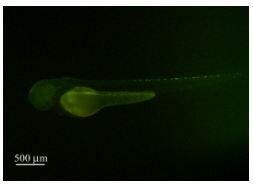	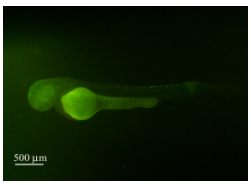	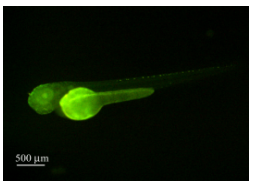
B	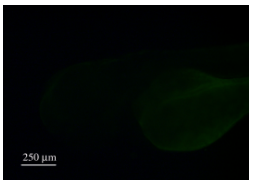	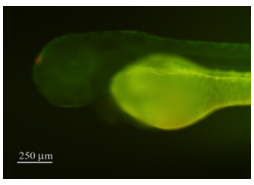	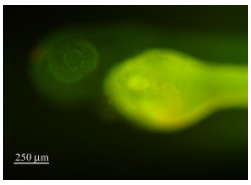	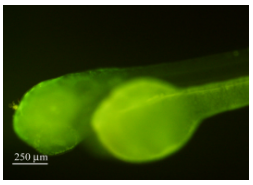
C		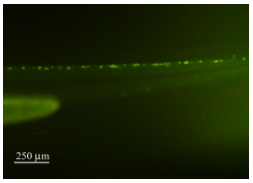	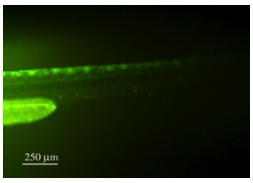	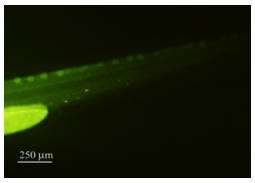
D	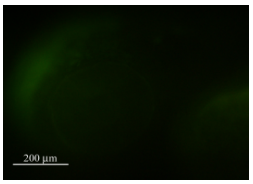	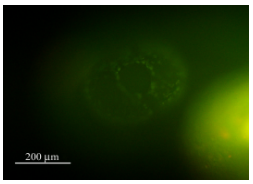	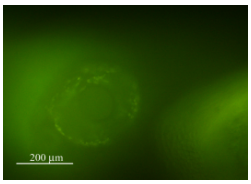	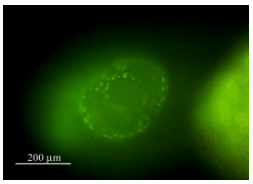

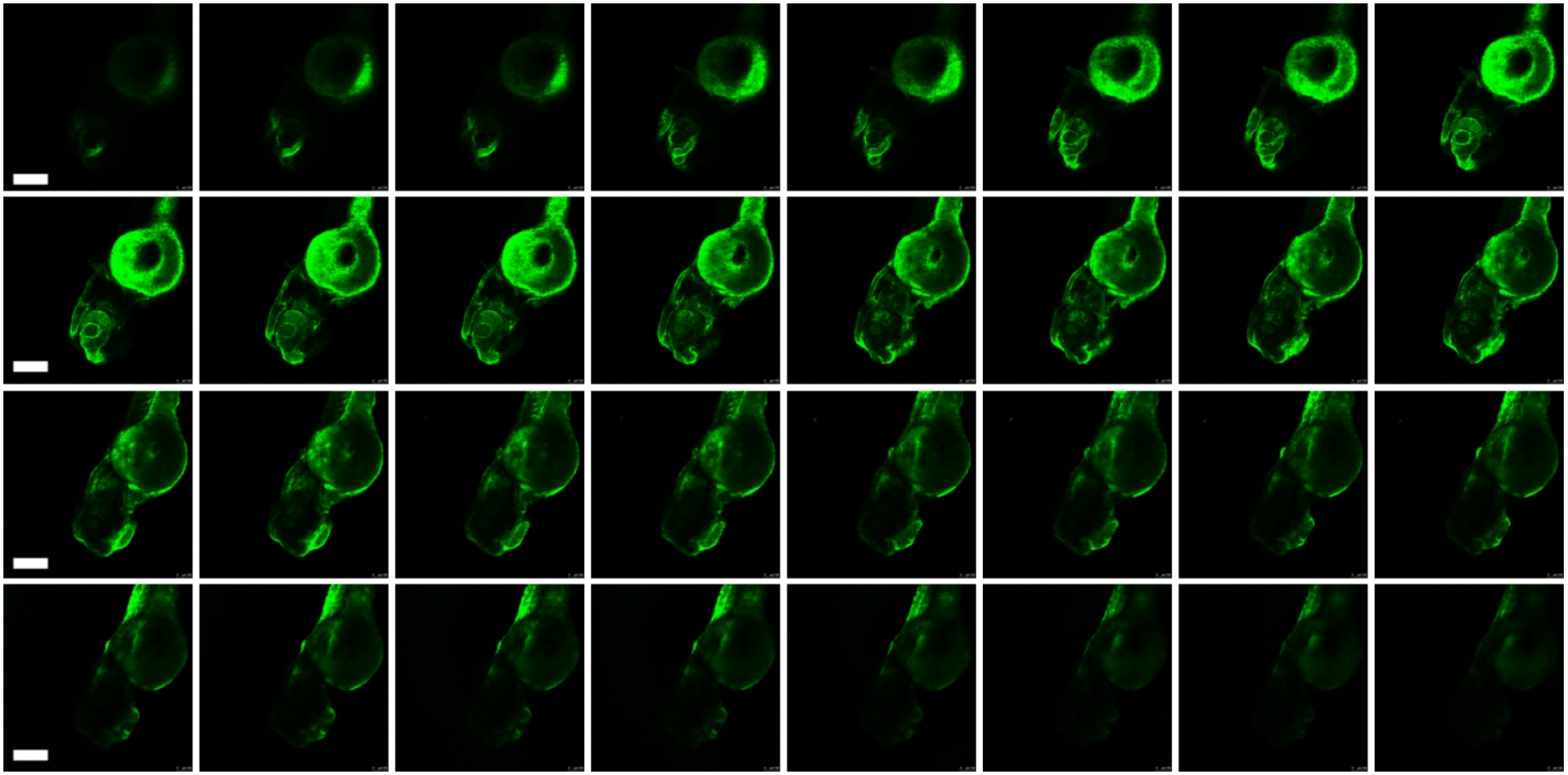

Fig. S10. Confocal images of zebrafish after incubated with ^{13}C-QDs at different scan-planes. Scale bar: 200 μm.

Supplementary References

1 (a) S. Zhu, Q. Meng, L. Wang, J. Zhang, Y. Song, H. Jin, K. Zhang, H. Sun, H. Wang, B. Yang, *Angew. Chem. Int. Ed.* 2013, **52**, 3953-3957; (b) Y.-Q. Zhang, D.-K. Ma, Y. Zhuang, X. Zhang, W. Chen, L.-L. Hong, Q.-X. Yan, K. Yu, S.-M. Huang, *J. Mater. Chem.* 2012, **22**, 16714-16718; (c) J. Lu, J.-X. Yang, J. Wang, A. Lim, S. Wang, K. P. Loh, *ACS Nano* 2009, **3**, 2367-2375.

2 (a) Y. Dong, R. Wang, H. Li, J. Shao, Y. Chi, X. Lin, G. Chen, *Carbon* **2012**, *50*, 2810-2815; b) Z.-C. Yang, X. Li, J. Wang, *Carbon* **2011**, *49*, 5207-5212.

3 (a) Z. Ma, H. Ming, H. Huang, Y. Liu, Z. Kang, *New J. Chem.* 2012, **36**, 861-864; (b) S. Liu, J. Tian, L. Wang, Y. Luo, J. Zhai, X. Sun, *J. Mater. Chem.* **2011**, *21*, 11726-11729.

4 F. Wang, X. Yang, L. Ma, B. Huang, N. Na, D. He, J. Ouyang, *J. Mater. Chem.* **2012,** *22,* 24597- 24604.

5 J. Wang, C.-F. Wang, S. Chen, *Angew. Chem. Int. Ed.* 2012, **51**, 9297-9301.

6 L. Cao, M. J. Meziani, S. Sahu, Y.-P. Sun, *Acc. Chem. Res.* 2012, **46**, 171-180.